

# Hosting Capacity of Distribution Networks for Controlled and Uncontrolled Residential EV Charging with Static and Dynamic Thermal Ratings of Network Components

As'ad Zakaria<sup>1</sup>, Chengyan Duan<sup>1</sup>, and Sasa DJokic<sup>1</sup>

<sup>1</sup>The University of Edinburgh

July 10, 2023

## Abstract

This paper proposes an approach to evaluate the loading limits of distribution networks due to increasing EV connections. It focuses on two parameters: after-diversity maximum demand (ADMD) and maximum daily energy demand (MDED). Using actual EV charging data from the UK, Monte Carlo simulations generate daily charging profiles, identifying ADMD, MDED, and seasonal variations. ADMD, MDED, and per-hour maximum EV charging demands are combined with UK residential load profiles before EV connection. Their maximum demands are assessed against thermal rating limits, establishing the network's hosting capacity (HC) for uncontrolled EV charging. To determine the maximum safe number of connected EVs, different scheduling methods for controlled EV charging are compared, considering per-hour maximum demand values, thermal limits, and MDED. This defines the network's HC for fully controlled EV charging. The approach is demonstrated on the IEEE 33-bus test network. Pre-EV residential demands are obtained from a UK MV substation, and ambient data is collected from a UK Met Office weather station. Results provide a range of network HC values for uncontrolled and controlled EV charging, representing lower and upper limits. These limits correlate with firm and non-firm network HC concepts and guide optimal network upgrades for exceeding these limits.

# Hosting Capacity of Distribution Networks for Controlled and Uncontrolled Residential EV Charging with Static and Dynamic Thermal Ratings of Network Components

A. Zakaria, C. Duan, S. Z. Djokic

School of Engineering, The University of Edinburgh, Edinburgh, Scotland, UK

E-mail: [Sasa.Djokic@ed.ac.uk](mailto:Sasa.Djokic@ed.ac.uk)

**Abstract:** The ongoing electrification of road transportation sector, which is expected to continue to strongly increase over the next years, will result in the connection of a significant number of electric vehicle (EV) chargers in LV and MV distribution networks, particularly in residential applications with on-board (“slow”) EV chargers. In order to evaluate loading limits of existing distribution networks for the maximum number of EV chargers that can be safely connected (commonly denoted as a network EV “hosting capacity”, HC), this paper introduces a general approach to determine one commonly used network design parameter (after-diversity maximum demand, ADMD) and one new parameter (maximum daily energy demand, MDED), which are both obtained from the load profiles of maximum per-hour demands for uncontrolled residential EV charging. The presented approach uses actual EV charging data from the UK as the inputs in Monte Carlo simulations to generate daily EV charging profiles for arbitrary numbers of EVs, enabling to identify related ADMD, MDED and per-hour maximum demand values, as well as their seasonal variations. The assessed ADMD, MDED and hourly maximum EV charging demands for uncontrolled EV charging are then combined with available UK residential daily load profiles before the EVs are connected (“pre-EV demands”), where their combined coincidental and noncoincidental maximum demands are evaluated against the static thermal rating (STR) and dynamic thermal rating (DTR) loading limits of network components (transformers and overhead lines), taking into account relevant weather/ambient conditions. This is denoted as a network HC for uncontrolled EV charging. Finally, evaluating the resulting per-hour maximum demand values against the STR and DTR loading limits and MDED values, allows to select one particular scheduling method for controlled EV charging, which gives the absolute maximum number of EVs that can be safely connected in the considered network, i.e., network HC for fully controlled EV charging. The presented approach is illustrated on the example of the IEEE 33-bus test network (modelled using typical UK network components), for the pre-EV residential demands taken from the recordings at an UK MV substation, and for ambient data taken from an UK Met Office weather station. Obtained results allow to evaluate the range of network EV HC values for uncontrolled and controlled EV charging, i.e., lower and upper HC limits, which can be correlated with the commonly used allocations of the firm and non-firm network HC, respectively.

## 1. Introduction and Brief Literature Review

The strong and widespread uptake of electric vehicles (EVs) will result in a substantial increase of demands in distribution networks (DNs), particularly in residential applications with on-board (“slow”) EV chargers. This new demand from EVs is in previous work approached as a significant challenge and as an opportunity for realising various demand management and balancing services [1–3]. The main concern is related to uncontrolled charging of a large number of EVs, which is generally assumed to coincide with the peak demand of the existing pre-EV loads, therefore likely resulting in network overloading. The term EV hosting capacity (HC) is often used to denote the maximum number of EVs that can be accommodated in a given DN [4]–[6], where impact of EVs on the DN is typically determined through the analysis of the resulting load profiles, i.e., combined demand of existing pre-EV loads and EV charging load associated with uncontrolled, or in some way controlled charging of EVs [5], [7–10].

One commonly used network design parameter for assessing the maximum coincidental demand of multiple instances of the same/similar type of the loads is after diversity maximum demand (ADMD), also known as demand factor [11–12]. In case of EVs, the ADMD of EV charging

loads is their coincidental maximum demand over a given period, taking into account diversity of EV demands and reflecting the fact that not all EVs will charge simultaneously.

While there is a large number of studies investigating impact of EV charging on DNs, only a few of these performed the analysis of EV ADMD values. The previous related work often focused only on the mean/average ADMD values, without evaluating the full ADMD ranges [13–14], what may result in an overestimation of the network EV HC, especially considering the likelihood of the higher EV demands than the mean ADMD values.

Research in [15] has quantified the ADMD of EVs in DN with multiple charging points, showing that ADMD allows for a realistic estimation of EV demands and helps to prevent oversizing of network components. However, a typical convergence of the ADMD values, i.e., the asymptotic ADMD result, which is expected for a sufficiently high number of EVs, was not demonstrated. Work in [16] considered the ADMD as a coincidence factor for EVs, using number of EVs and their charging power and charging energy as variables, indicating that ADMD strongly depends on the number of EVs, with lower dependency on EV battery capacity. However, temporal variations of ADMD and their impact on the network were not investigated in more detail.

This paper introduces a general approach to determine the ADMD of an arbitrary number of EV charging loads, which is obtained from the available measurements of uncontrolled residential EV charging demands. The paper demonstrates that the time at which the peak EV charging demand occurs varies with the number of connected EVs, which effectively prevents to simply add ADMD-based maximum EV charging demand to the peak demand of the pre-EV loads to obtain their combined peak demand. Therefore, the loading limits and HC of considered DN for the maximum number of EVs that can be safely connected are in the paper determined from the maximum per-hour demands of uncontrolled residential EV charging, while one new energy-based parameter, maximum daily energy demand (MDED), is used for the evaluation of possible controlled EV charging schemes.

The IEEE 33-bus test network is used as an example to illustrate presented approach for evaluating EV HC in terms of the loading limits of network components. This test network is modelled using typical UK transformer and overhead line (OHL) components. The transformer's static thermal rating (STR) [17-18] is assumed to be its rated power (maximum continuous power transfer capacity). As the transformer STR does not account for the effects of ambient temperature, load variations and other factors that impact its operating conditions (i.e., operational temperature limits), the paper also uses dynamic thermal rating (DTR) for a more accurate evaluation of transformer loading conditions [19-24]. To the best of authors' knowledge, only one paper in existing literature considered the DTR of transformers when analysing impact of EVs on DN networks, [21], where assumed load profiles of 40 EVs are used for the analysis.

This paper also analyses EV HC with respect to both STR and DTR limits of the OHLs in the considered DN [26-27]. In a few previous references, [25], [28-29], the DTR of the OHLs is used in the analysis with EVs, reporting substantial increase of the EVs that can be connected without violating thermal limits. However, these studies did not consider the aggregate impact and diversity of EV charging profiles.

Two general approaches can be used to manage increased EV charging demands, as reviewed in [2], [30–32]. The first is to increase network loading capacity by upgrading the network. However, this can be expensive and may not always be feasible. The second approach is to implement some demand management scheme, i.e., to control and shift the EV charging load from peak demand period to off-peak hours, which is in this paper denoted as a controlled EV charging (term EV scheduling is also used in existing literature). It should be noted that there is a very high number of possible scheduling schemes for controlled EV charging, which further increases with the increase of the EVs that should be charged (it is basically a combinatorial problem, with the scheduling of the target number of EVs within the available time periods and based on the required EV demand).

In terms of a large number of possible scheduling schemes for controlled EV charging, there is a significant previous work on optimal EV charging, e.g., in [29], where optimisation of EV charging considered voltage constraints, or in [30], where stochastic optimisation considered uncertainty of EV arrival and departure times and available renewable energy sources, or in [31], where charging of EVs in parking lots also considered available renewable energy sources, or in [2] and [32], where metaheuristic methods were implemented for optimal scheduling of EV charging.

Instead of evaluating a very large number of possible scheduling methods, this paper presents a simple and robust energy-based approach, which is derived from the ADMD analysis and gives the absolute maximum number of EVs that can be safely connected in the considered network with known or assumed pre-EV load profiles, and assuming full control of EV charging. This can be approached as the maximum non-firm HC, or upper HC limit, while the HC limit for the uncontrolled EV charging can be approached as a firm HC, or lower HC limit, representing fully uncontrolled EV charging.

The main contributions of this paper are:

- Establishment of a general approach for assessing actual daily load profiles and envelope of maximum hourly demands for the uncontrolled EV charging load (including Level 1 and Level 2 EV chargers).
- Evaluation of conventional (single) ADMD value and hourly ADMD values for arbitrary number of EVs under uncontrolled EV charging.
- Formulation of a simple and robust methodology, which uses one new indicator, maximum daily energy demand (MDED), to identify maximum number of EVs that can be connected under fully controlled EV charging.
- Introduction of a new methodology for determining combined DTR limits of transformers and OHLs.
- Evaluation of the EV HC allocations for uncontrolled EV charging (firm HC) and fully controlled EV charging (non-firm HC) based on the STR limits and coincidental and noncoincidental DTR limits, as well as combined total pre-EV and EV charging demands.

## 2. Input Data for the Analysis: Existing (Pre-EV) Demands and EV Charging Demands

### 2.1 Existing Load Data (Pre-EV Demand)

Typical variations in loading conditions before the EVs are connected (i.e., “pre-EV demands”) are identified from hourly recordings of power demands of a residential Scottish MV distribution substation, available for a period from 2007-2012 [33]. Fig. 1 shows normalised six-year daily load profiles (light blue curves), with absolute maximum demand occurring at 19:00 hours (1 p.u. value), indicated by a red square. Fig. 1 also shows other hourly maximum demands of interest: envelope of maximum demands at each hour (red dashed line with red “x” symbols), hourly demands on the day of maximum demand (dotted dark blue line) and two daily load profiles coinciding with the days of maximum EV charger demands for Level 1 and Level 2 chargers (see next sections), indicated with black solid circles and black hollow squares.

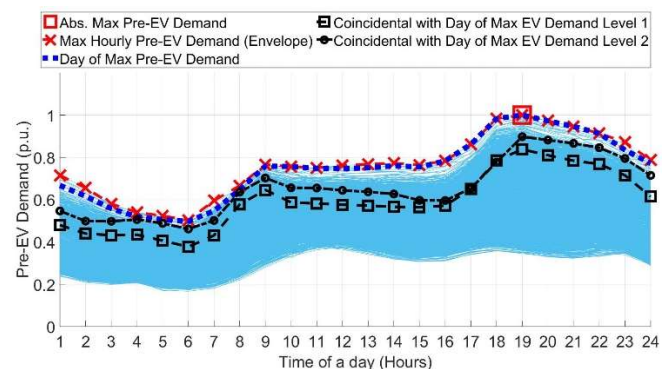


Fig. 1 Hourly pre-EV load profiles (six years of recording).

## 2.2 EV Load Data (Uncontrolled EV Charging)

The measured EV demands were sampled from a field trial in [34], spanning from 2014-2015 and representing uncontrolled EV charging. In this trial, all EVs were of the same type, [35], featuring battery capacity of 24 kWh and on-board Level 1 single-phase charger with a rating of 3.5 kW (1 p.u. power for Level 1 charging) and a near-unity power factor.

The EVs selected for the analysis are those for which hourly charging demands were continuously recorded for an entire year and for which related time and date stamps were available. This resulted in the selection of around 200 EVs, representing the EVs with the highest occurrences of charging events between June 2014 and July 2015 (with all EVs having a plug-in factor of at least 30%). As it was observed that some EVs had demands exceeding 3.5 kW, which was likely due to voltage-dependency of their power demands, the EVs with up to 10% higher demands (i.e., up to 3.85 kW, or 1.1 p.u.) were also included in the analysis. The EV charging data are presented in the form of time series, comprising 24 hourly values for each day, and 365 daily profiles over the course of a year.

To assess the impact of a newer Level 2 on-board 7 kW EV charger in the same type of EV, which was also upgraded with a 48-kWh battery charger, it is assumed that all EVs will travel the same distances under the identical conditions throughout the year (requiring the same amounts of energy from the battery for the same journeys), therefore resulting in around 50% shorter charging times for EVs equipped with Level 2 chargers, compared to EVs with Level 1 chargers.

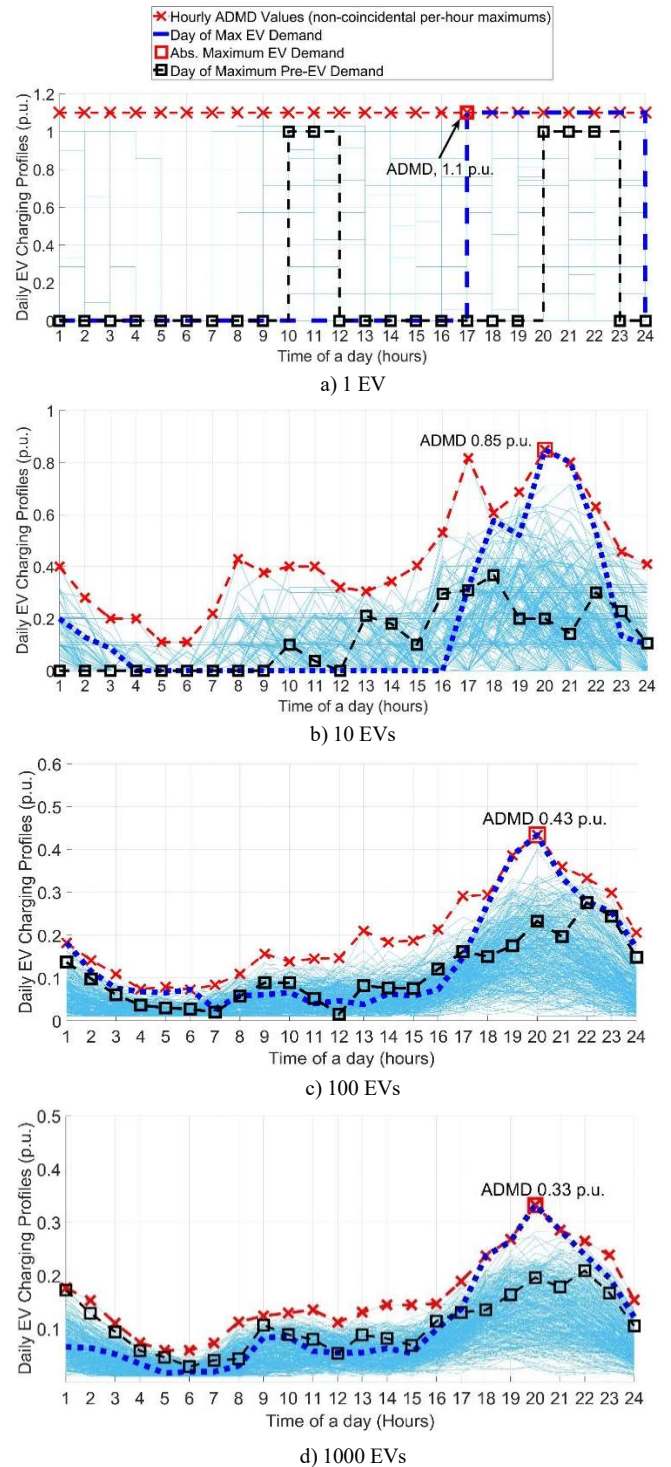
## 3. Daily Load Profiles, ADMD and MDED values for Uncontrolled EV Charging

### 3.1 Generation of Daily Load Profiles for Arbitrary Number of EVs

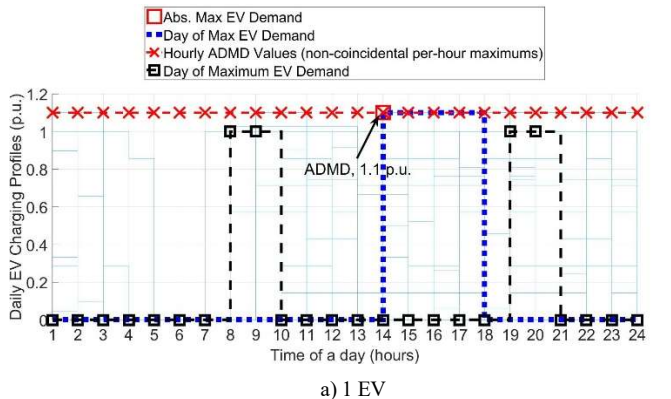
After selecting 200 EVs with hourly recordings available for a whole year, Monte Carlo simulation (MCS) approach is used to generate aggregate coincidental demands (daily load profiles) of the pre-specified number of EVs, where each charging event for each EV from the available dataset is considered independently. In that way, recorded individual daily EV charging profiles of a specified number of EVs, denoted as  $N$ , over a one-year period (365 days) are randomly combined, summed up for each day and normalised using a base of 3.5 kW as 1 p.u. for Level 1 EV chargers, while a base of 7 kW is used for Level 2 EV chargers. The MCS runs are repeated 1000 times, typically resulting in the standard deviation error below 0.1% [16].

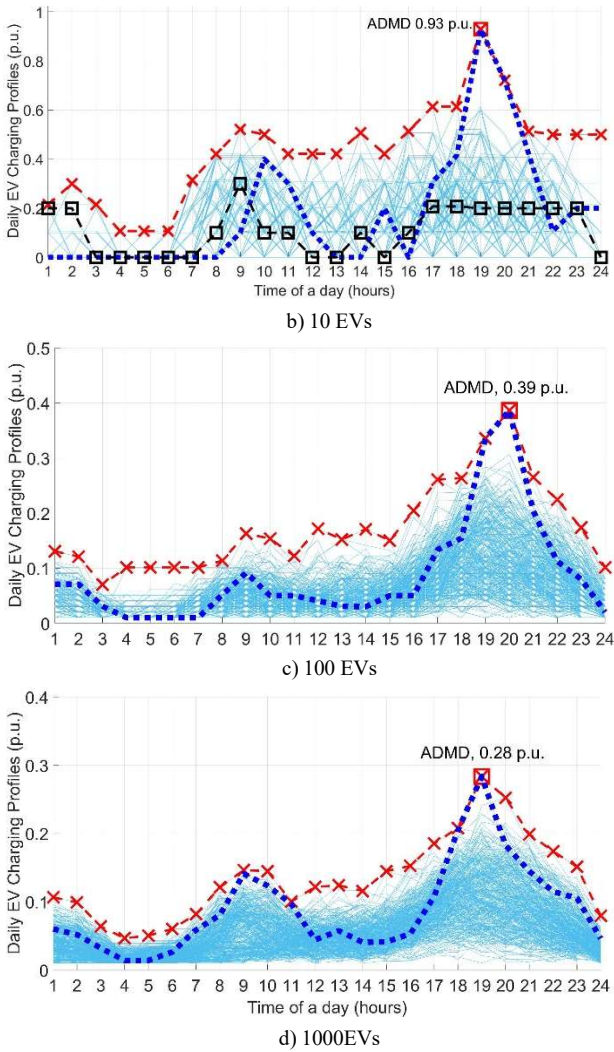
In cases where the number of EVs exceeds the available 200 recorded EV charging profiles, resampling with replacement is implemented, assuming homogeneity among the available EV charging demands.

Fig. 2 and Fig. 3 illustrate generation of daily EV charging load profiles, for  $N = 1; 10; 100;$  and 1000 EVs with Level 1 and Level 2 EV chargers, respectively (the highest 1% load profiles from the 1000 MCS runs are shown in both figures). The light-blue curves represent individual daily EV charging profiles, from which following characteristic demands and load profiles can be identified: a) absolute maximum coincidental demand (corresponding to a conventional single ADMD value), b) envelope of maximum demands for each hour of the day (i.e., “hourly ADMD” values, corresponding to noncoincidental hourly maximum demands), c) load profile for a day of the maximum EV demand (when ADMD is reached), and d) EV charging load profile coincidental with the day of maximum pre-EV demand (see previous section).



**Fig. 2** Hourly EV Charging Profiles and ADMD for 1, 10, 100 and 1000 EVs with Level 1 chargers





**Fig. 3** Hourly EV Charging Profiles and ADMD for 1, 10, 100 and 1000 EVs with Level 2 chargers

### 3.2 Load Profiles of Maximum EV Charging Demands

As indicated in Fig. 2 and Fig. 3, the MCS-generated load profiles allow to extract two characteristic maximum hourly EV charging demands: a) noncoincidental maximum hourly values, i.e., envelope of maximum hourly demands at each of the 24 hours of the day (indicated by red dashed line and symbol “x”), and b) coincidental hourly demands on the day the ADMD is reached (on the day of maximum EV charging demand, indicated by a dotted dark blue line). Fig. 4 and Fig. 5 show these as daily load profiles of maximum hourly EV charging demands, and daily load profiles for actual days of maximum EV charging demands, respectively, plotted as 3D graphs for uncontrolled charging of up to 3000 EVs.

Fig. 4 and Fig. 5 show that the time of the day at which the conventional single ADMD value (the absolute maximum EV charging demand) occurs is different for different numbers of EVs (indicated with a red dashed line). The time-dependent changes of ADMD prevent simple combining of ADMD values of EV charging demand and pre-EV load demand, as this will give neither the correct maximum combined demand (their coincidental peak demand), nor the correct time at which it occurs. For example, the time of the peak pre-EV load demand is 19:00 hours, while the time of the peak demand of EV charging load changes in the range 19:00-21:00 hours, depending on the number of EVs and use of Level 1 or Level 2 type of the charger.

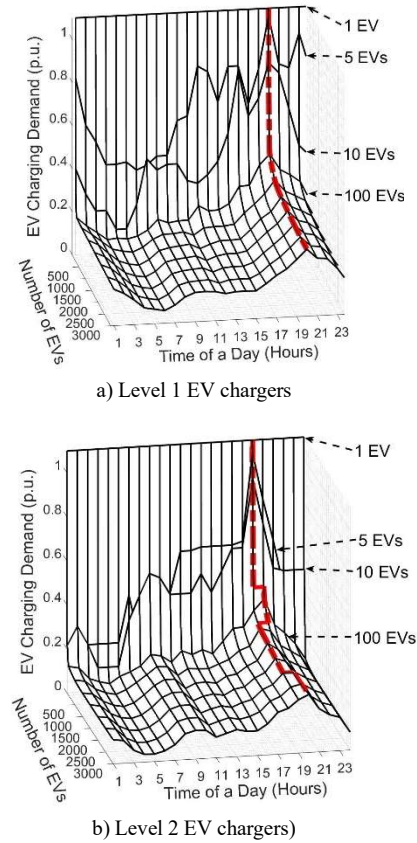


**Fig. 4** Load profiles of maximum hourly EV charging demands

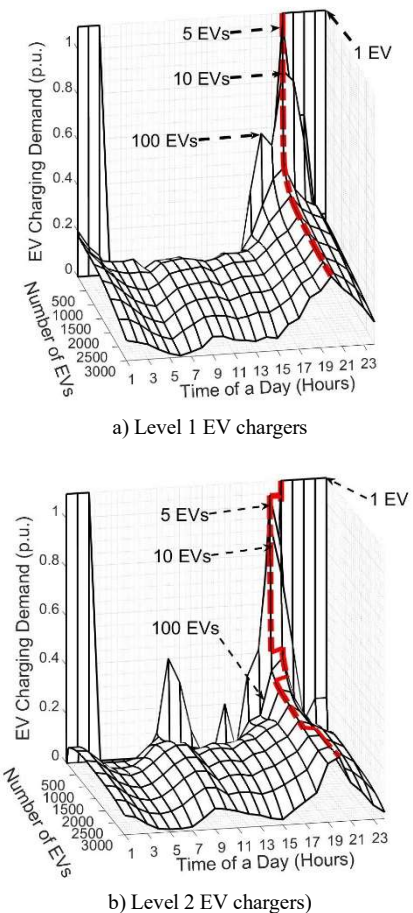


**Fig. 5** Load profiles for actual days of maximum EV charging demands

### 3.3 Conventional ADMD and Hourly ADMD Values

After the MCS-based daily load profiles are generated, Fig. 2-Fig. 5, various values of ADMD can be identified, including: minimum, 1<sup>st</sup> percentile, 5<sup>th</sup> percentile, 25<sup>th</sup> percentile, mean (50<sup>th</sup> percentile), 75<sup>th</sup> percentile, 90<sup>th</sup> percentile, 95<sup>th</sup> percentile, 99<sup>th</sup> percentile, and maximum ADMD values. The analysis is conducted separately for Level 1 and Level 2 EV chargers, and for the numbers of aggregated EVs varied in groups of N=1; 5; 10; 50; 100; 200; 1000; 2000; and 3000.

The ADMD value for a specific number of EVs can be expressed as follows:

$$ADMD_{t \rightarrow T, N, m \rightarrow M} = \max \left[ \frac{1}{N} \sum_{n=1}^N (P_{EV(t,n,m)}) \right] \quad (1)$$

where:  $ADMD_{t \rightarrow T, N, m \rightarrow M}$ , is the ADMD of combinations of  $N$  EVs, with  $n \in N$  in ranges from  $N = 1; 5; 10; 50; 100; 200; 1000; 2000;$  and  $3000$ , for a given period,  $t$  to  $T = 365$  days, with the 24-hourly step intervals in each day. The intermediate ADMD values are summed up and averaged over observations at time  $t$ , considering the specified number of EV combinations,  $N$ . The MCS runs are repeated for samples  $m \rightarrow M$ , where  $M$  is equal to 1000.

Fig.6a and Fig.6b (left) show the ADMD results, where light-blue lines represent 1000 ADMD values obtained from 1000 MCS runs. For a single EV ( $N=1$ ), its ADMD will always be at its maximum charging demand, which, as discussed previously, is set at 1.1 p.u. Different numbers of EVs result in varying ranges of ADMD values, with wider ranges observed for the combinations roughly below 100 EVs. For example, random combinations of 10 Level 1 EV chargers return a range of 0.4 p.u.-0.9 p.u. between the minimum and maximum ADMD values. As the number of EVs increases, the ranges of ADMD values narrow down, "converging" towards the asymptotic ADMD value for the

maximum number of EVs considered (3000). The ADMD curves for different numbers of EVs are plotted as interpolated nonlinear fits, based on calculated values for varying EV numbers,  $N$ .

It can be further observed that the ADMD values for Level 2 EV charging (ranging from 0.21 p.u. to 0.25 p.u. for 3000 EVs) are lower than the ADMD values for Level 1 EV charging (ranging from 0.28 p.u. to 0.35 p.u. for 3000 EVs). This difference is attributed to the shorter duration of charging and therefore lower coincidence of charging events for EVs with Level 2 chargers, as they require half of the charging time for Level 1 EV chargers (assuming same trips and same energy from the EV batteries for these trips). This can also be seen in the magnified inset plots in Fig. 6 (left).

However, while the ADMD plots in Fig. 6a and Fig. 6b (left) show relatively small differences in per-unit values, it is important to note that the difference in base values between Level 1 and Level 2 EV chargers results in substantial differences in absolute demand values. For instance, the differences between the mean and maximum values for 3000 EVs with Level 1 and Level 2 chargers are 284 kW and 525 kW, respectively. Finally, it can be clearly seen that the use of the mean ADMD values to represent the maximum coincidental demands from EV chargers could significantly underestimate possible demand (and therefore impact) of EV charging load, suggesting that the absolute maximum ADMD values, or sufficiently high percentile values (e.g., 99<sup>th</sup> or 95<sup>th</sup> percentiles) should be used.

Fig. 6a and Fig. 6b (right) show the maximum hourly EV charging demands from which single conventional ADMD values, indicated by red-dashed lines, can be seen as a "side view" from the Y-axis, while the remaining values give "hourly ADMD values" for up to 3000 EVs.

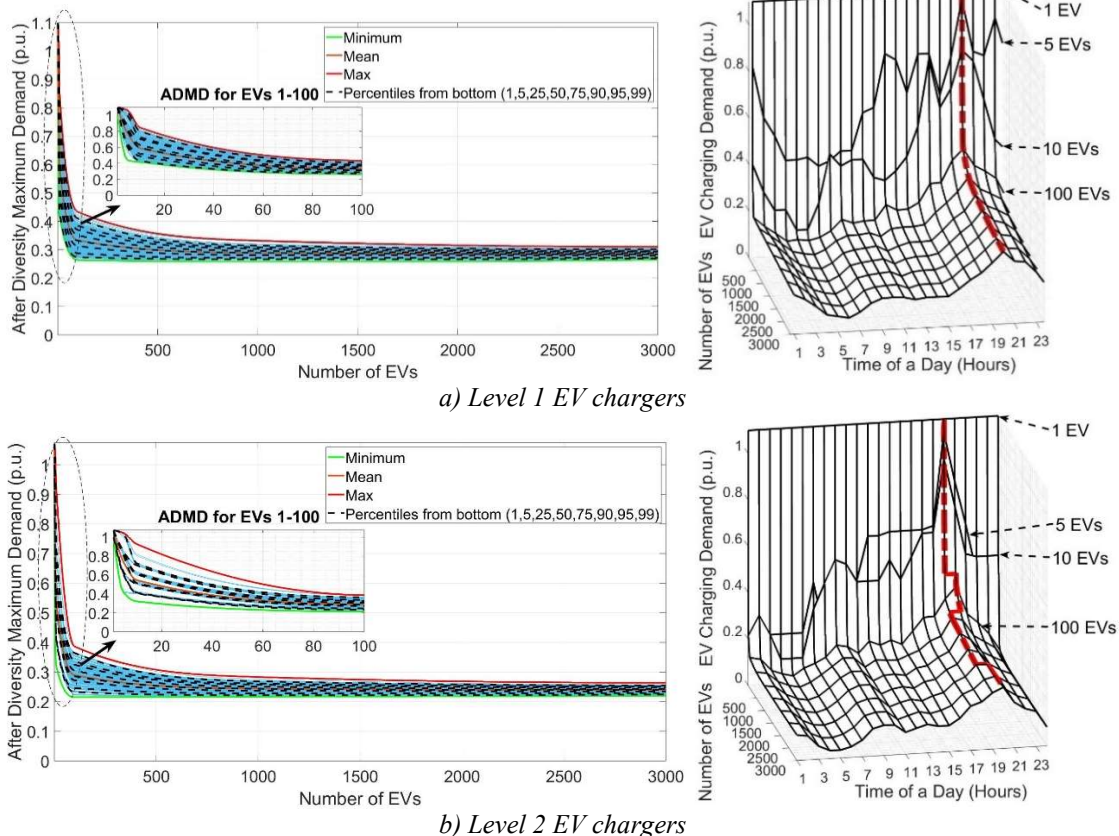


**Fig.6** The ADMD percentile values (left) and hourly maximum EV charging demands (right) for up to 3000 EVs

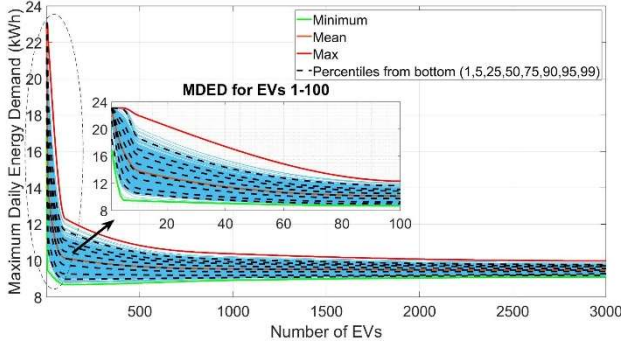
### 3.4 Deriving kW Demand from Per-Unit ADMD Values

When the ADMD is known for a given number of EVs,  $N$ , the corresponding coincidental maximum power demand in kW,  $P_{N,max}$ , can be determined as:

$$P_{N,max} = ADMD_{t \rightarrow T, N, max} \cdot N \cdot L \quad (2)$$

where:  $ADMD_{t \rightarrow T, N, max}$ , is the maximum (100<sup>th</sup> percentile) ADMD for a given period  $t$  to  $T$ ,  $N$  is the number of EVs, and  $L$  is the charging level (Level 1 or Level 2). Fig. 7 depicts the changes of the EV maximum active power demand (in kW) based on the number of connected EVs, which is highly non-linear for the first 100 EVs and then increases almost linearly (as the corresponding ADMD values in Fig. 6 converge).

### 3.5 Maximum Daily Energy Demand (MDED)



a) Level 1 EV chargers

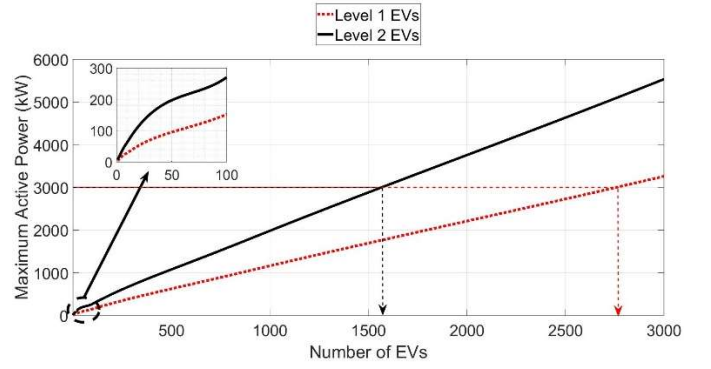
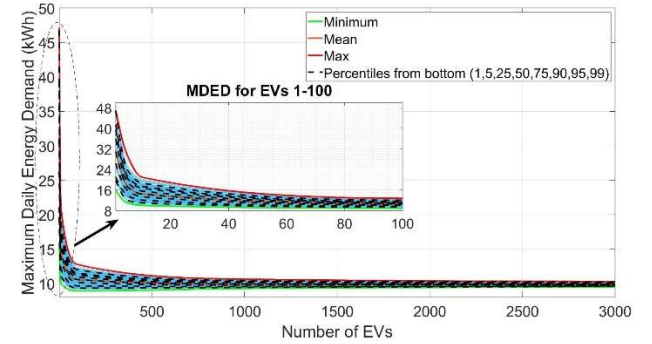


Fig. 7  $P_{N,max}$  for Level 1 and Level 2 EV chargers



b) Level 2 EV chargers

Fig. 8 Maximum daily energy demand (MDED) values

Although it is highly unlikely that the uncontrolled EV charging will be allowed for any significant number of connected EVs, the uncontrolled EV charging reveals one very important information: the energy required for charging, which should be provided regardless of what EV scheduling (or EV demand shifting) scheme will be implemented. In other words, it is assumed that the uncontrolled EV charging truly reflects the actual energy demand of EV owners/users for charging their EV batteries, as required for their trips.

As the presented analysis uses hourly EV charging demands, the required maximum daily energy demand (MDED) can be simply obtained as the sum of maximum hourly power demands from maximum EV charging load profiles, for specific number of EVs, as expressed in (3).

$$MDED_{N,m \rightarrow M} = \max \left[ \frac{1}{N} \sum_t \sum_{n=1}^N (P_{EV}(t,n,m)) \right] \quad (3)$$

where:  $MDED_{N,m \rightarrow M}$ , is the maximum daily energy demand calculated “per EV”, as illustrated in Fig. 9, and with all subscripts as defined in (1). This is similar to ADMD, and when maximum daily energy demand should be calculated for a specific number of EVs,  $N$ , the corresponding value  $E_{N,max}$  (for the maximum 100<sup>th</sup> percentile values of demands) is calculated from (3) by multiplying MDED with  $N$ :

$$E_{N,max} = MDED_{N,max} \cdot N \quad (4)$$

where:  $MDED_{N,max}$  is the maximum/100<sup>th</sup> percentile MDED value for a given number of EVs,  $N$ .

The MDED is introduced in this paper as a new metric, as it is a very useful constraint or requirement that should be used in specifying optimal scheduling of EV charging demands, as shown in the further analysis in Section 6.4.

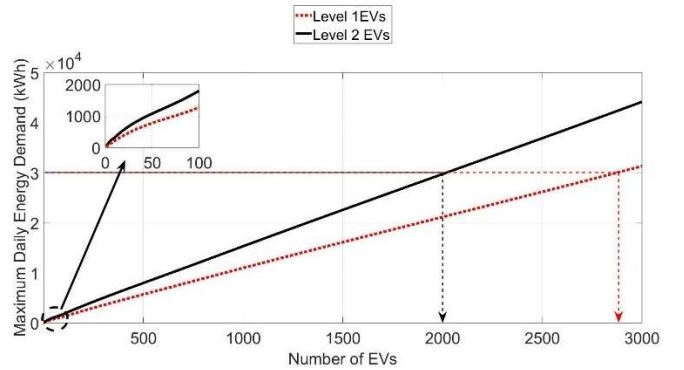
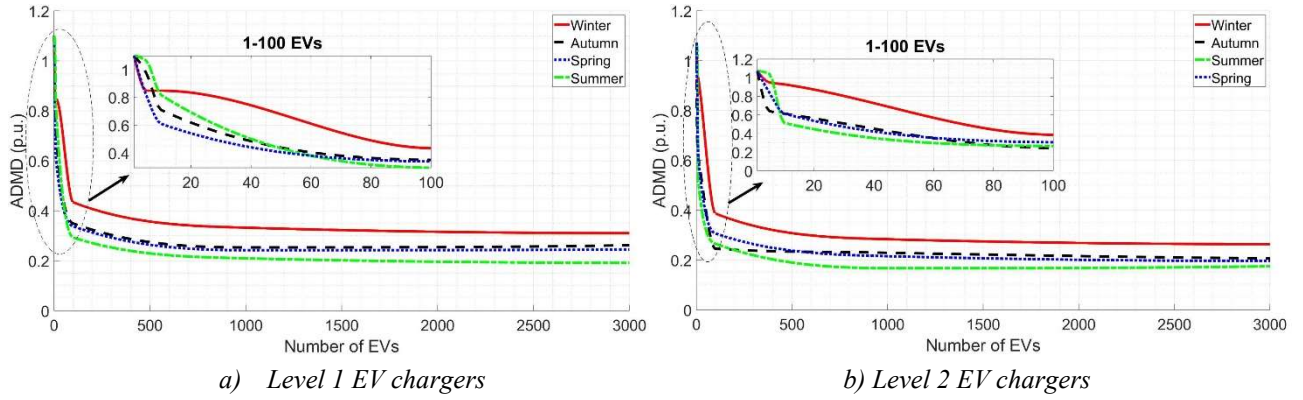


Fig. 9 MDED values for Level 1 and Level 2 EV chargers

### 3.6 Seasonal Variations in ADMD and MDED Values

As the ambient conditions (e.g., temperature, length of the day, etc.) vary in different seasons, it is likely that the ADMD and MDED values will exhibit seasonal variations. Fig. 10 illustrates the variations in ADMD values in four seasons in the UK (obtained from uncontrolled EV charging data from a UK field trial), where the highest ADMD is in winter, followed by autumn and spring, while the lowest ADMD is in summer. This is expected, as the EV batteries will additionally discharge in winter, due to the lower ambient temperatures and heating of the interior of the EVs, as well as use of EV headlights due to the shorter daylight hours [36]. Fig. 11 shows corresponding seasonal variations of the MDED values, which are similar to the ADMD variations.

The increased EV charging demand in the UK in winter coincides with the peak of the typical residential UK pre-EV demand, but it should be noted that there may be different relationships in other countries, e.g., in countries with hot climate, where the peak pre-EV demand occurs in summer.



**Fig. 10** Seasonal variations of ADMD values for Level 1 (left) and Level 2 (right) EV chargers.

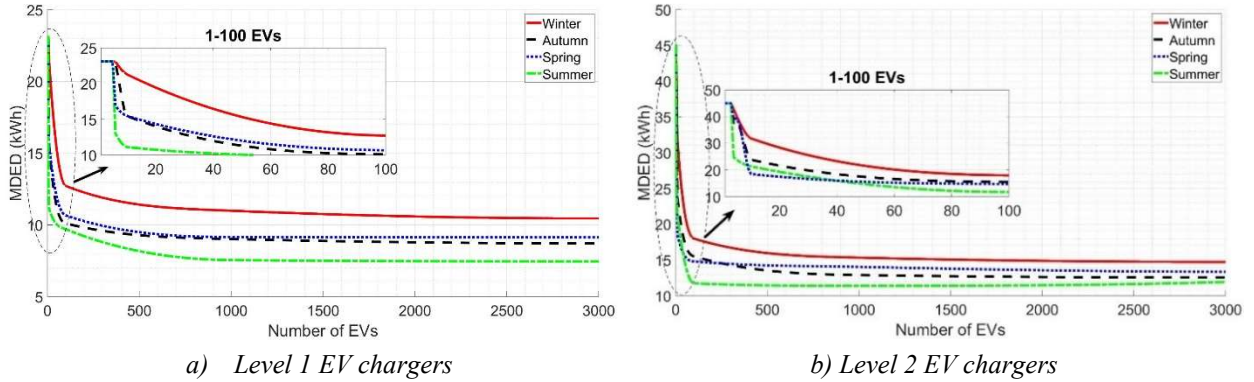


**Fig. 11** Seasonal variations of MDED values for Level 1 (left) and Level 2 (right) EV chargers

### 3.7 Combined Demand of Pre-EV Load and EV Charging Load

The previous sections presented analysis of uncontrolled EV charging demands in residential applications, for arbitrary number of EVs with Level 1 and Level 2 on-board (“slow”) chargers. The analysis allowed to evaluate maximum hourly EV charging demands in form of daily load profiles, from which commonly used conventional single ADMD value (with corresponding percentiles) and “hourly ADMD” values are identified, together with the related MDED values.

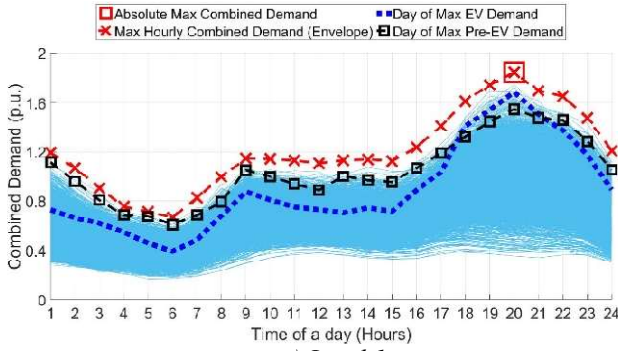
As also discussed, two sets of results are obtained during the evaluation of the maximum demands for uncontrolled EV charging: a) noncoincidental maximum hourly values, represented by the envelope of maximum hourly demands, and b) coincidental hourly demands on the day of peak EV charging load, when ADMD is reached, as shown in Fig. 4 and Fig. 5. An obvious question is which of these two sets of maximum EV charging demands should be used for assessing the combined maximum demand when additional EV load is connected together with the existing pre-EV load?

The most conservative approach would be to use the envelope of hourly maximum demands for both pre-EV load and EV charging load (or some high percentile values of these). Fig. 1 indicates that there are small differences between the envelope of hourly maximum demands and hourly demands on the day of peak pre-EV load (i.e., day of peak demand also features the highest hourly demands). Fig. 4 and Fig. 5, however, indicate larger differences between the envelope of the noncoincidental (not on the same day) maximum hourly demands and coincidental hourly demands on the day of the peak EV charging load. Although this result is expected, as the EV charging demand cannot be consistently high throughout the all hours of the day, this does not exclude the possibility of a (close to) maximum hourly EV charging demand at a specific hour occurring at any given day,

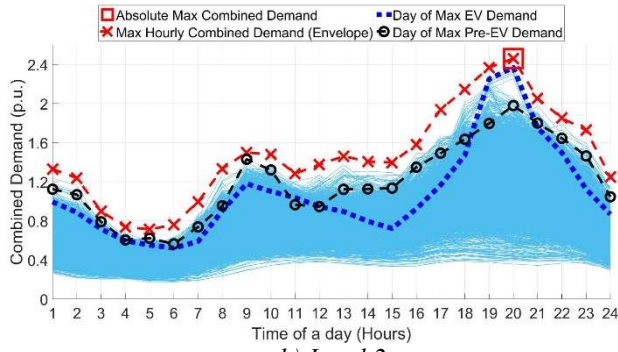
including the day on which pre-EV demand at that hour is also maximum, or close to the maximum values. Therefore, even if a more detailed probabilistic analysis of the coincidence of the demands of the pre-EV load and EV charging load is performed on available datasets, the most conservative approach would be to assume that the maximum EV charging demand at any specific hour could occur when the pre-EV demand at that hour is also at the maximum value.

Accordingly, for assessing the maximum combined total demand, which is the primary objective of both the ADMD analysis and network EV HC evaluation, this paper suggests three following approaches:

- 1) The use of the envelopes of noncoincidental hourly maximum demands for both pre-EV load and EV charging load (the most conservative approach), illustrated in Fig. 12 with red dashed lines with “x” symbols. The example shown is for 3000 EVs with Level 1 and 2 chargers, where 1 p.u. corresponds to the maximum demand of the pre-EV load of 3.72 MW, representing 1785 residential customers.
- 2) The use of the combined total coincidental demand, where the day of the maximum pre-EV demand is selected first, and then the corresponding hourly EV charging demands on that day are added, indicated by a black dashed lines with hollow squares in Fig. 12. The corresponding day of EV charging demand is the one with maximum demands from 1000 MCS runs.
- 3) The use of the combined total coincidental demand, where the day of the maximum EV charging demand is selected first (maximum from 1000 MCS runs), and then the corresponding hourly pre-EV demands on that day are added (the same calendar day, but with the maximum demand from available 6 years of data), indicated by a dotted dark-blue line in Fig. 12.



a) Level 1



b) Level 2

Fig. 12 Combined pre-EV demand and demand of 3000 EVs

#### 4. Test Network, Transformer and OHL Data

The network used for the analysis is the IEEE 33-bus network from [37], Fig. 13, with the base voltage modified to 11 kV, in order to allow for the modelling of typical UK network components. The total active/reactive power demands of pre-EV load are 3.72 MW / 2.3 MVar. All buses, except Bus 1, are available for the connection of EVs. The OHL (Table 1) is a 6/1 single layer aluminium conductor steel reinforced (ACSR) Type P for all feeders, with STR of 80 °C and 382 A, corresponding to 6.84-7.71MVA (for  $\pm 10\%$  voltage variations from nominal value) [38]. The substation transformer (Table 2) is a 6.3 MVA ONAN (oil natural, air natural) type, with 35/10.5 kV voltages and OLTC control [37]. The nameplate rated MVA of transformer is considered as its STR limit.

Table 1 Parameters of modelled OHL [38]

|   |        |
|---|--------|
| Normal Thermal Ratings <sup>a</sup> (A) | 390    |
| Overall Diameter (mm)                   | 14.31  |
| DC Resistance at 25°C (Ohms/km)         | 0.2618 |
| AC Resistance at 25°C (Ohms/km)         | 0.2697 |
| AC Resistance at 75°C (Ohms/km)         | 0.3829 |

a. Ambient temperature of 35°C, solar irradiance of 0 W/m<sup>2</sup>, wind speed of 0.6 m/s, and attacking angle of 90 °

Table 2 Parameters of modelled transformer [39]

|  |       |
|--|-------|
| Rated MVA/ STR (MVA)                   | 6.3   |
| Cooling type                           | ONAN  |
| No-load losses (kW)                    | 4.5   |
| Load losses rated (kW)                 | 36.7  |
| Winding HST rise at rate power (°C)    | 65    |
| Max. ambient temperature (°C)          | 45    |
| Height <sup>b</sup> (m)                | 1.62  |
| Length (m)                             | 4.1   |
| Width (m)                              | 2.6   |
| Thickness of transformer side wall (m) | 0.01  |
| Number of radiators <sup>c</sup> (-)   | 5     |
| Radiator area (m <sup>2</sup> )        | 22.05 |

b. Transport height is used to eliminate the height of the bushing of the transformer

c. Five active radiators and one radiator in reserve

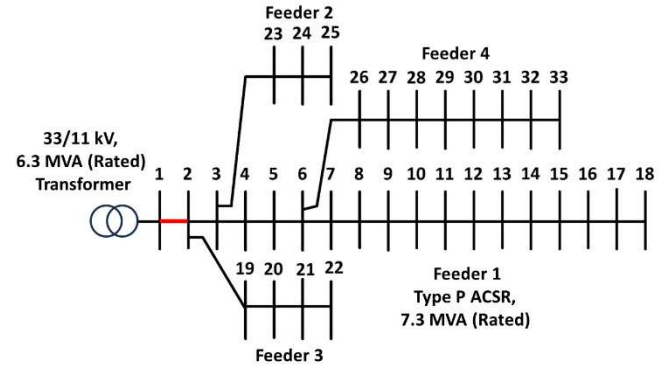
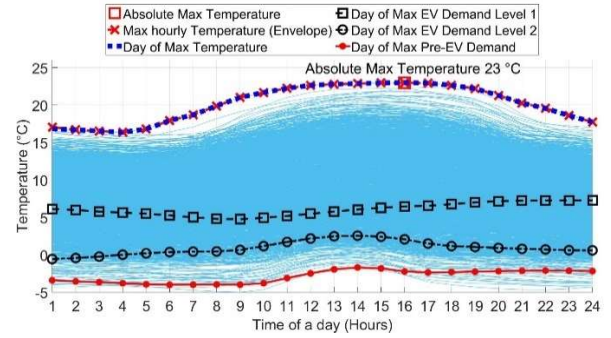


Fig. 13 The IEEE 33-bus test distribution network

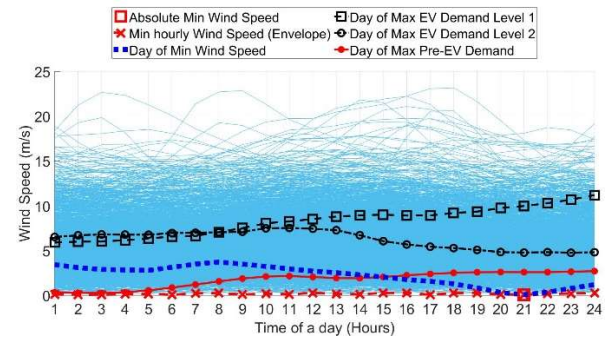
### 5. Ambient Conditions and DTR Calculations

#### 5.1 Weather Data

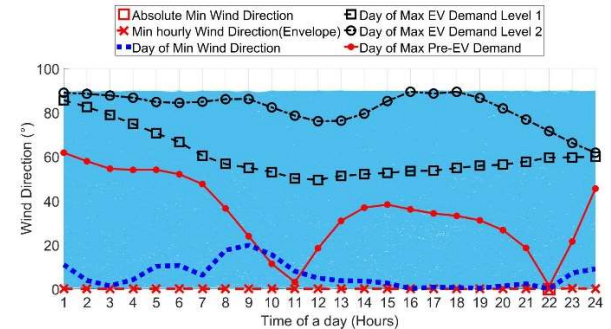
The required inputs to determine hourly DTRs of OHL and transformer are weather data, which are extracted from [40]. Fig. 14 shows hourly variations in ambient conditions for a location in the UK over a six-year period (2007-2012). The absolute highest and lowest values, along with corresponding hourly maximum and minimum values, are indicated, which will serve as input parameters for determining the minimum DTRs of the network components. For the ambient conditions coincidental with the days of maximum EV charging demands and pre-EV load demands, the corresponding daily ambient parameters are also plotted and indicated in Fig. 14.



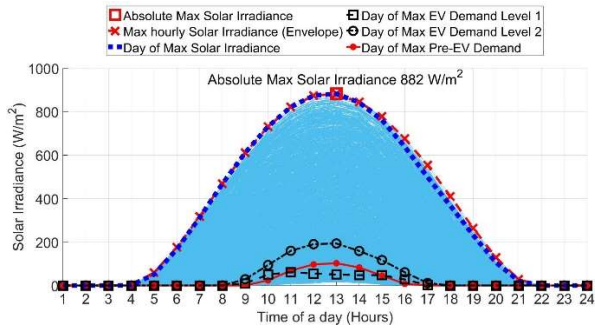
a) temperature variations



b) wind speed variations



c) normalised wind direction (0° to 90°) variations



d) solar irradiance variations

Fig. 14 Ambient conditions over six years (UK location)

### 5.2 DTR of Overhead Line (OHL)

Thermal balance equations outlined in [41] are used to calculate the changes in loading limits, i.e., dynamic thermal rating (DTR) of the considered OHL (further details in [42]), with weather conditions from the previous section.

It should be noted that the OHL loading limits are typically given as the maximum allowed currents, i.e., in amps (A), while thermal limits for transformers are typically given in MVA. Therefore, the upper and lower MVA limits of OHL can be obtained from the upper and lower limits for

Table 3: The STR and DTR limits and ambient conditions for considered OHL.

| OHL Parameters and Limits | Abs. Min DTR | STR Summer | STR Winter | Min DTR Summer | Min DTR Winter | 1 <sup>st</sup> Percentile DTR | 5 <sup>th</sup> Percentile DTR |
|---------------------------|--------------|------------|------------|----------------|----------------|--------------------------------|--------------------------------|
| Temperature (°C)          | 23.0         | 14         | 4          | 20.8           | 4.6            | 11.7                           | 5.9                            |
| Wind Speed (m/s)          | 0            | 0.5        | 0.5        | 4.6            | 0.8            | 8.1                            | 2.0                            |
| Wind Att. Angle (°)       | 0            | 12         | 12         | 6.5            | 1              | 37                             | 74                             |
| Solar Irr. ( $W/m^2$ )    | 882          | 0          | 0          | 852            | 157            | 1                              | 0                              |
| 0.9 p.u. (MVA)            | 4.82         | 6.17       | 6.56       | 4.98           | 6.42           | 7.19                           | 8.42                           |
| 1 p.u. (MVA)              | 5.35         | 6.85       | 7.29       | 5.53           | 7.13           | 7.99                           | 9.3                            |
| 1.1 p.u. (MVA)            | 5.89         | 7.53       | 8.02       | 6.08           | 7.84           | 8.79                           | 10.29                          |

The daily variations of DTR values (with 1-hour steps) for the considered OHL (Table 1) are plotted in Fig. 15 for ambient conditions from Fig. 14. The absolute minimum DTR is marked with a red-square and it can be seen that the minimum hourly DTRs in both seasons are not coincidental with the maximum pre-EV demand and day of maximum EV charging demands (for both Levels 1 and 2 chargers). The minimum summer hourly DTR values (red line “x” symbol) are lower than STR values (green-dotted line) only during the mid-day, while minimum hourly DTRs in winter (blue dotted line with diamond symbol) is roughly equal to the winter STR.

### 5.3 DTR of Transformer

The thermal rating of the transformer depends on the hot spot temperature (HST) limit, which can be calculated as defined in [19]. To determine the DTR of the transformer, it is essential to be consistent with the definition of the DTR of the OHL (see previous section), i.e., the DTR of the transformer should be calculated for the steady state operating conditions and thermal equilibrium state. The presented analysis assumes that the HST of the transformer with thermally upgraded insulation will not exceed 110°C (98°C for transformer with non-thermally upgraded insulation) for average 24-hour ambient temperature of 30°C and under continuous loading with full rated power. The summary of the calculated DTR and STR values for considered transformer is given in Table 4.

the allowed voltage variations. Accordingly, the OHL DTRs in MVA in Table 3 are listed for nominal voltage of 1 p.u., but also for lower value of 0.9 p.u. and upper value of 1.1 p.u.

For the EV HC analysis, two seasonal STR values, one noncoincidental absolute minimum DTR value, and two coincidental minimum hourly DTR values are used, as shown in Table 3. The Absolute minimum DTR is the lowest possible value of DTR derived from the noncoincidental combination of the worst ambient conditions (highest temperature and solar irradiance, and lowest wind speed). The STR values for summer and winter are typically given by the DN operators (DNOs), as e.g., in [43]. For minimum hourly DTR values, weather data are further searched in summer and in winter, to identify coincidental (i.e., actual simultaneously recorded weather conditions for which) the minimum DTR values in two seasons are obtained. Finally, the calculated minimum DTR values in Table 3 are “relaxed” by taking 1<sup>st</sup> and 5<sup>th</sup> percentile values, as the minimum coincidental DTRs may have a (very) low probability. However, this is shown for illustration only, and relaxed DTR values for both OHL and transformer are not used for the EV HC analysis in this paper. Also, 1 p.u. voltage is used for the calculation of the OHL DTR limits in MVA.

Fig. 16 shows the daily variations of transformer DTR values, where the minimum hourly DTRs in summer and winter are always higher than the STR (green-dotted-line), indicating that the STR is a more conservative limit. Similar to OHL limits, the minimum DTR values are not coincidental with neither EV charging demand, nor with pre-EV demand.

Table 4: The STR and DTR limits and ambient conditions for considered transformer.

| Transf. Parameters and Limits | STR  | Min DTR Summer | Min DTR Winter | 1 <sup>st</sup> Perc. DTR | 5 <sup>th</sup> Perc. DTR |
|-------------------------------|------|----------------|----------------|---------------------------|---------------------------|
| Temperature (°C)              | /    | 23.0           | 12.6           | 18.0                      | 15.8                      |
| 1 p.u. (MVA)                  | 6.30 | 6.68           | 7.27           | 6.93                      | 7.05                      |

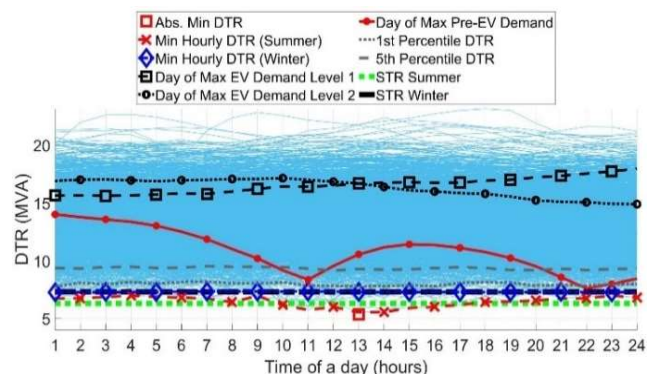


Fig. 15 The STR and variations of DTR values (OHL)

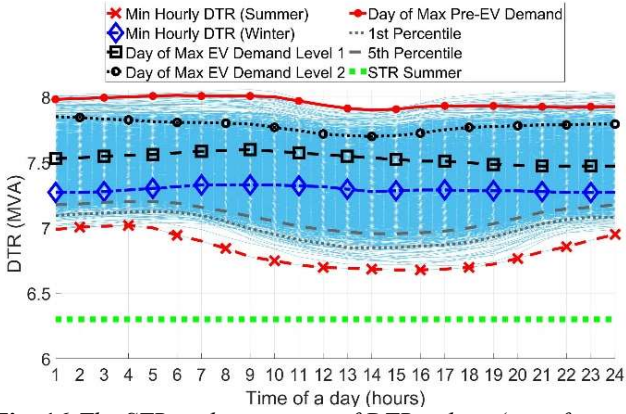


Fig. 16 The STR and variations of DTR values (transformer)

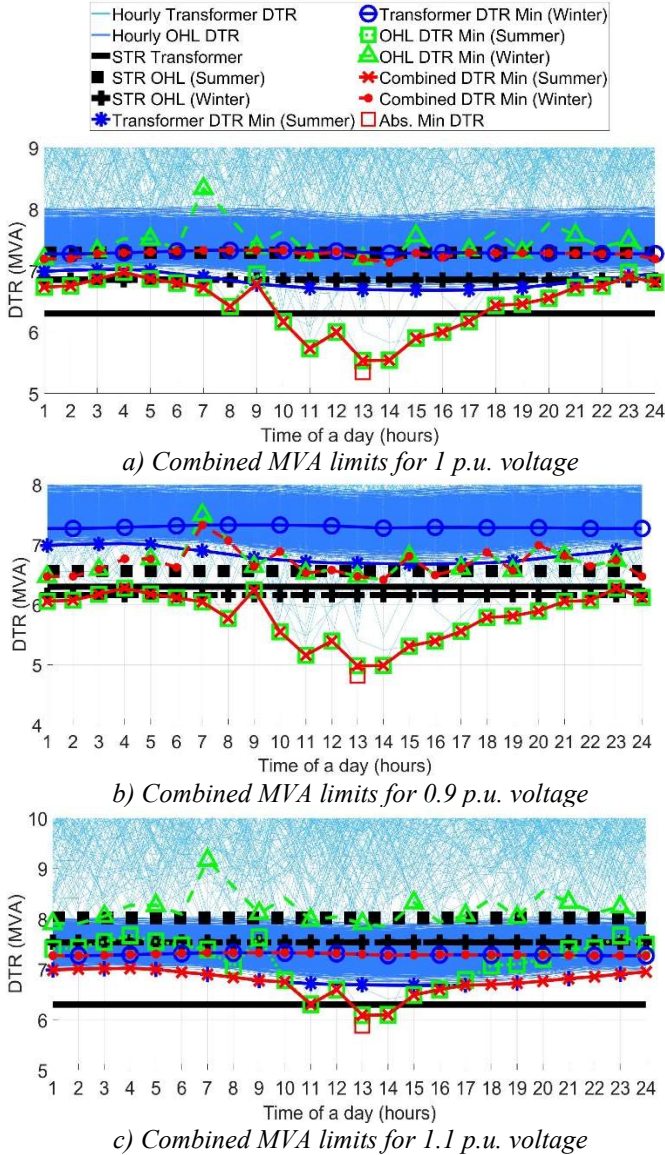


Fig. 17 Combined transformer-OHL minimum DTR limits

#### 5.4 Combined Transformer-OHL Minimum DTR Limits

Fig. 17 illustrates the results for the combined OHL and transformer hourly minimum DTR limits, with absolute minimum DTR values indicated by a red hollow square, as well as the STR and minimum seasonal DTR limits.

It can be seen from Fig. 17a, where OHL MVA limits are calculated for 1 p.u. voltage, that absolute minimum DTR value is constrained by the OHL, rather than transformer. If

the STR values are used, the loading limit is constrained by the transformer, not by the OHL STRs in both summer and winter (6.3 MVA for transformer vs 6.85 MVA and 7.29 MVA for OHL). The minimum hourly DTR values (red dashed line with “x” symbol) are predominantly limited by the OHL, but for some hours are very close to minimum transformer DTRs.

However, Fig. 17b and Fig. 17c show the OHL loading limits in MVA for lower and upper allowed voltages of 0.9 p.u. and 1.1 p.u., respectively, illustrating that based on the loading conditions, voltage drops in the network and applied voltage regulation/control functionalities, the minimum DTR of transformer may be the constraining loading limit, not the minimum DTR of the OHL (Fig. 17c). The analysis in the further text assumes 1 p.u. voltage and uses combined OHL-transformer MVA limits from Fig. 17a for the evaluation of the network EV HC.

## 6. Considered Case Studies and HC Allocations

### 6.1 Considered EV Penetration Levels and Mixes

The presented analysis assumes that all busses, except Bus 1, are available for connecting EVs, and that both pre-EV load and newly connected EV charging load are proportionally distributed at all buses. The ADMD of residential pre-EV load is taken from [44], where it is given as 2.27 kW per household (for one residential customer). The network HC is evaluated with respect to the maximum expected EV penetration, assuming that all petrol/diesel cars are replaced with EVs, where the figure of 1.68 EVs per household is adopted based on [45]. For the selected network with specified pre-EV demands, this gives the maximum number of EVs as:

$$N_{\text{Household}} = \frac{P_{\text{total\_pre-EV}}}{2.27} \quad (5)$$

$$N_{\text{EV}} = N_{\text{Households}} \cdot 1.68 \quad (6)$$

where:  $N_{\text{Households}}$  is the total number of households in the network,  $P_{\text{total\_pre-EV}}$  is the maximum pre-EV charging demand in kW, and  $N_{\text{EV}}$  is the total number of EVs in the network. For the considered network and pre-EV demand, the total number of EVs is around 2750 for 168% EV penetration (i.e., 1.68 EVs per household). The EVs are distributed proportionally in the network based on the given active power demands at individual buses of IEEE 33-bus network in [37]:

$$n_{i,\text{EV}} = \frac{1.68 \text{ EV}}{\text{Househol}} \cdot \frac{1}{2.27} \frac{\text{Household}}{\text{kw}} \cdot p_{i,\text{total\_pre-EV}} \quad (7)$$

where:  $n_{i,\text{EV}}$  is the number of EVs at bus,  $i$  and  $p_{i,\text{total\_pre-EV}}$  is the total pre-EV demand at bus,  $i$  in kW, [37].

Additionally, analysis is performed for all EVs equipped with Level 1 on-board chargers, for all EVs equipped with Level 2 on-board chargers, and for EVs equipped with mixes of Level 1 and 2 on-board chargers, as shown in Table 5.

Table 5: Different mixes of EVs with Level 1 & 2 chargers

| Scenario | Level 1 | Level 2 |
|----------|---------|---------|
| Level 1  | 100%    | 0%      |
| Mix 1    | 80%     | 20%     |
| Mix 2    | 60%     | 40%     |
| Mix 3    | 40%     | 60%     |
| Mix 4    | 20%     | 80%     |
| Level 2  | 0%      | 100%    |

## 6.2 Network Constraints

The analysis of the combined total demands of pre-EV load and EV charging load from the previous section does not take into account active and reactive power losses in the network. Although these losses can be estimated and added to the total combined demands (typically, losses in DNs are 5%-10% of the supplied total demands), a more accurate and common way to calculate losses is to perform standard power flow analysis. In this paper, steady state three-phase ac power flow is carried out using [46], with relevant constraints described in (8-17). The two main network components that are of most interest is substation transformer at Bus 1 and the highest loaded line from Bus 1 to Bus 2 (Fig. 13).

$$P_{i+1,t}^l = P_{i,t}^l - i \frac{(P_{i,t}^{l,2} + Q_{i,t}^{l,2})}{V_{i,t}^2} - p_{i+1,t} \quad (8)$$

$$Q_{i+1,t}^l = Q_{i,t}^l - x_i \frac{(P_{i,t}^{l,2} + Q_{i,t}^{l,2})}{V_{i,t}^2} - q_{i+1,t} \quad (9)$$

$$V_{i+1,t}^2 = V_{i,t}^2 - \frac{2(r_i P_{i,t}^l + x_i Q_{i,t}^l)}{V_{i,t}} + (r_i^2 + x_i^2) \frac{(P_{i,t}^{l,2} + Q_{i,t}^{l,2})}{V_{i,t}^2} \quad (10)$$

$$p_{i,t} = P_{i,t}^d + P_{i,t}^{EV} \quad (11)$$

$$q_{i,t} = Q_{i,t}^d \quad (12)$$

$$V_{min} < V_{i,t} < V_{max} \quad (13)$$

$$tap_{min} < tap_t < tap_{max} \quad (14)$$

$$S_{l,t}^{(i,j)} \leq STR_l \quad (15)$$

$$S_{l,t}^{(i,j)} \leq DTR_{l,t} \quad (16)$$

$$(P_{l,i,j})^2 + (Q_{l,i,j})^2 \leq (S_{l,max})^2 \quad (17)$$

$$\forall i \in N_i, \forall t \in T, \forall l \in L$$

Equation (8) and (9) describe the active and reactive power flows in line  $l$ , from bus  $i$  to bus  $i+1$ ; equation (10) shows the voltage at bus  $i$  and its adjacent bus, bus  $i+1$ ;  $P_{i,t}^l$  and  $Q_{i,t}^l$  are active and reactive load flow of line,  $l$  from bus  $i$  to bus  $i+1$  at time  $t$ ;  $P_{i,t}^d$  and  $Q_{i,t}^d$  are the active and reactive pre-EV load demands at bus  $i$ ;  $P_{i,t}^{EV}$  is EV active power demand at bus  $i$ ;  $p_{i,t}$  and  $q_{i,t}$  are power injections at bus  $i$ ;  $V_{i,t}$  is the voltage of bus  $i$ ;  $r_i$  and  $x_i$  are series impedance of branch from bus  $i$  to bus  $i+1$ ;  $tap_t$  in (14) is the tap position at time,  $t$

The tap position is set to change when undervoltage occurs. The voltage upper limit  $V_{max}$  is set to be 1.1 p.u., while the lower limit  $V_{min}$  is 0.9 p.u. in (13). Equations (13-17) represent inequality constraints determined by technical limits of distribution networks. Equation (14) provides limits of on-load tap setting of the 33/11kV transformer and equation (13) give the limits on bus voltages. Equations (15-16) correspond to the apparent power,  $S_{l,t}^{(i,j)}$  and power flow constraints for each branch, where  $STR_l$  or  $DTR_{l,t}$  limits of the branch (OHL or transformer) from bus  $i$  to bus  $i+1$  at time,  $t$ .

## 6.3 Uncontrolled EV Charging

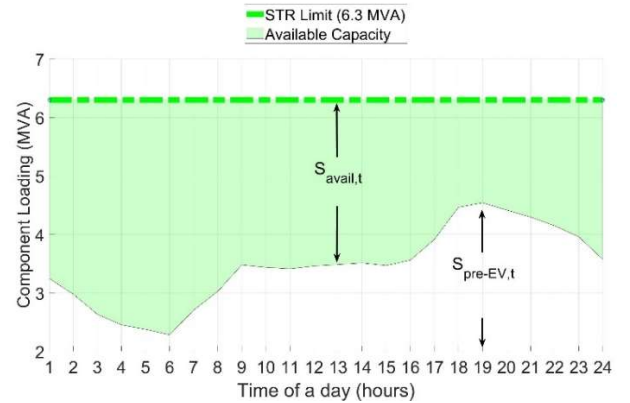
The analysis of the network EV HC is conducted in two stages: first for uncontrolled EV charging, and then for (fully) controlled EV charging. Each stage is further divided into noncoincidental and coincidental cases, based on the loading limits of network components and combined total demands of pre-EV load and EV charging load.

The uncontrolled EV charging demand is analysed using the hourly ADMD values, as previously described, helping to identify daily load profiles as the envelope of maximum hourly demands for arbitrary number of uncontrolled EVs. This approach enables to calculate HC (i.e., the number of EVs that can be accommodated for uncontrolled EV charging) based on the difference between available loading/thermal limit and maximum pre-EV demand.

For controlled EV charging, it is assumed that all uncontrolled EV demands can be shifted and fully adjusted (e.g., by the DNO, or by the aggregator) from any time of the day at which they occur, to any other available/suitable time of the day, as necessary or suitable in terms of available loading capacity between the applied STR or DTR limit and pre-EV demand. This is described next.

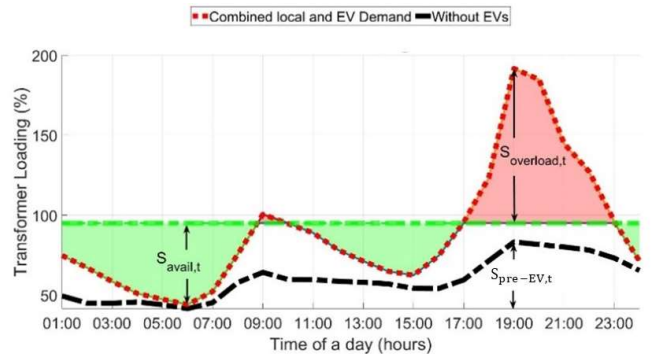
## 6.4 Controlled EV Charging: Maximum Number of EVs that Can Be Connected Based on MDED values

Fig. 18 shows the day of the maximum pre-EV demand and STR limit, where the green-shaded area denotes available capacity for connecting new loads without overloading the network. Accordingly, if a new EV charger demand can be controlled to completely fits in the green areas, this will determine the maximum possible number of EVs that can be connected in this network (some ‘‘safety margin’’ can be added, e.g. up to 90% of the STR limit). As the green area is equivalent to the amount of energy in MVAh that can be safely supplied, the newly introduced MDED indicator can be used to directly calculate number of EVs that can be connected assuming full control of their charging.



**Fig. 18 Fully controlled EV scheduling (for maximum number of EVs) on a day of maximum pre-EV demand, STR limit**

As an example, Fig. 19 further illustrates how uncontrolled EV charging, resulting in network overloading, can be controlled, in order to allow for the connection of the same number of EVs, but with shifted demand for charging.



**Fig. 19 Illustration of scheduling maximum EV demand**

The scheduling the highest possible number of EVs that can be connected for given pre-EV demand and applied STR/DTR limits is achieved when available capacity/area  $A_{avail}$  is used (“filled in”) with controlled EV charging daily energy demand, so that the loading of network components is exactly at their STR/DTR limits at all times,  $t$  to  $T$ . The “available area” and “overloaded area” are defined as:

$$A_{avail} = \sum_t^T S_{avail_t} \quad (18)$$

where:  $S_{avail_t}$  is the available capacity (e.g., minimum of the combined OHL and transformer loading limits) at any given time,  $t$ , in MVA, and the  $S_{overload_t}$  is the amount of overloading above the available MVA capacity at any given time,  $t$ ,  $S_{avail_t}$

$$S_{avail_t} = STR - S_{pre-EV_t} \quad (19)$$

$$S_{avail_t,DTR} = DTR_t - S_{pre-E_t} \quad (20)$$

where:  $S_{pre-E_t}$  is the pre-EV demand in MVA at a time,  $t$ . Equations (19) and (20) show that both STR and  $DTR_t$  limits can be used.

The objective of this EV scheduling is to find the amount of daily maximum EV energy demand,  $E_{N,max}$ , that will exactly fill-in the available capacity  $A_{avail}$ . For every time of the day,  $t$  to  $T$ , the corresponding available active power for EV connection,  $P_{avail_t}$ , is derived from its available apparent power  $S_{avail_t}$ , as expressed in (21), and summed throughout the day:

$$\sum_t^T P_{avail_t} = \sqrt{\sum_t^T S_{avail_t}^2 - \sum_t^T Q_{pre-EV_t}^2} - \sum_t^T P_{pre-EV_t} \quad (21)$$

Afterwards,  $P_{avail_{t \rightarrow T}}$  is proportionally distributed in the network according to (7), taking into account corresponding active power losses,  $P_{losses_{t \rightarrow T}}$  and reactive power losses,  $Q_{losses_{t \rightarrow T}}$ , which are obtained from power flow analysis with given number of EVs:

$$P_{avail_{t \rightarrow T}} = \frac{\sum_t^T P_{avail_t}}{\sqrt{\sum_t^T S_{avail_t}^2 - (\sum_t^T Q_{pre-EV_t} + \sum_t^T Q_{losses_t})^2} - (\sum_t^T P_{pre-EV_t} + \sum_t^T P_{losses_t})} \quad (22)$$

The calculated sum of hourly available active powers for EV connection throughout the day  $\sum_t^T P_{avail_t}$  is the maximum daily energy available for EV charging,  $E_{N,avail}$ :

$$E_{N,avail} = \sum_t^T P_{avail_{t,new}} \quad (23)$$

After maximum daily energy available for EV charging,  $E_{N,avail}$  is obtained, the corresponding number of EVs that can be connected can be simply taken from the MDDED plot in Fig. 9. For example, if  $E_{N,avail} = 30,000$  kWh is available, that would allow to connect around 2800 EVs with Level 1 chargers, and around 2000 EVs with Level 2 chargers, assuming that they are fully controlled, as described here.

## 7. Results

Once the thermal/loading limits of network components have been determined and combined demands of pre-EV load and EV charging load (for specified number of EVs) are established, the HC of the network can be assessed. The analysis assumes that the uncontrolled EV charging

represents the allocation of “firm HC”, while controlled EV charging represents the allocation of “non-firm HC”. The HC cases for uncontrolled and controlled EVs are defined as follows.

### Noncoincidental (NC) Cases:

- Noncoincidental Absolute Minimum HC: Absolute maximum EV charging demand is combined with the absolute maximum pre-EV demand, for both STR and absolute minimum noncoincidental DTR limits.
- Noncoincidental Hourly Minimum HC: Envelope of maximum hourly EV charging demand is combined with the envelope of maximum hourly pre-EV demands, using STR or hourly minimum DTR limits.

### Coincidental Cases:

- Coincidental Minimum HC: Day of maximum EV charging demand is combined with the coincidental hourly pre-EV demands, using STR or hourly minimum DTR limits.

### 7.1 Uncontrolled EV Charging: Firm EV HC

The numbers of EVs that can be connected for uncontrolled EV charging (firm EV HC) are plotted in Fig.19a. These cases are summarized as follows:

- Abs. NC DTR Min - Maximum EV demand combined with NC maximum pre-EV demand with Abs. Minimum DTR (red- coloured bar-plot)
- NC STR Min - Maximum EV demand combined with NC maximum pre-EV demand using STR limit (pink-coloured bar-plot)
- NC Winter DTR Min - Maximum Winter EV demand combined with NC maximum pre-EV winter demand using Hourly Minimum Winter DTR limits (green-coloured bar-plot)
- NC Summer DTR Min - Maximum Summer EV demand combined with NC maximum summer pre-EV demand using Hourly Minimum Summer DTR limits (green-coloured bar-plot)
- Coincidental Winter DTR Min - Maximum EV demand combined with coincidental pre-EV Winter demand using Hourly Minimum Winter DTR limit (purple-coloured bar-plot).
- Coincidental Summer DTR Min - Maximum EV demand combined with coincidental pre-EV Summer demand using Hourly Minimum Summer DTR limit (purple-coloured bar-plot).

The result in Fig. 20a clearly shows that the network EV HC is dependent on the levels of charging, with Level 1 EV chargers having higher EV HC. As the charger mixes change towards Level 2, a reduction of firm EV HC values can be noticed in all scenarios.

The results for “Abs. NC DTR Min” case are too conservative and unrealistic, as the related weather and loading conditions have extremely low probability, if any, to occur. However, if there are no detailed weather data except maximum/minimum measurements, and if there are no detailed recordings of loading conditions except peak demands, this may be the only network EV HC that can be calculated. Comparing firm EV HC results for STR and DTR limits, the STR limit (transformer rated MVA) also did not occur in analysis, and it may be also too conservative.

When considering DTR limits in each season, although the combined lower limits of summer DTR is much lower

(Fig. 17), the EV charger demand in the UK in summer is lower than in the winter (Fig. 11). On the other hand, the increase in EV demand during winter is more pronounced than the change in the minimum seasonal DTR. Therefore, the NC seasonal DTR is more than doubled for summer in every scenario, compared to winter.

The coincidental analysis of DTR is more realistic, and shows an increase in network EV HC compared to results for NC cases. If coincidental EV charger demands and pre-EV demands are used, the actual combined total demand is much lower than the NC total combined demands, resulting in higher network EV HC (with a higher EV HC in summer). The NC summer DTR scenario can host more EVs than the coincidental winter DTR scenario. For these reasons, it is important for DNOs to carefully examine opportunities

offered by the higher DTR limits of network components in winter, as well as the lower EV charger load and pre-EV load in summer in devising optimal control schemes. In addition, types and mixes of EV charger types (Level a or Level 2) that are to be supplied, should be also monitored.

### 7.2 Controlled EV Charging: Non-Firm EV HC

The network EV HC results for controlled EV charging (non-firm HC) are plotted in Fig. 20b. For all cases, significant increase in EV HC is observed across all cases. **Although the trend remains the same as the uncontrolled EV charging**, there is even more **significant increase in EV HC in summer**, as the decrease of EV charging demands in summer are more pronounced than decrease in DTR limits.

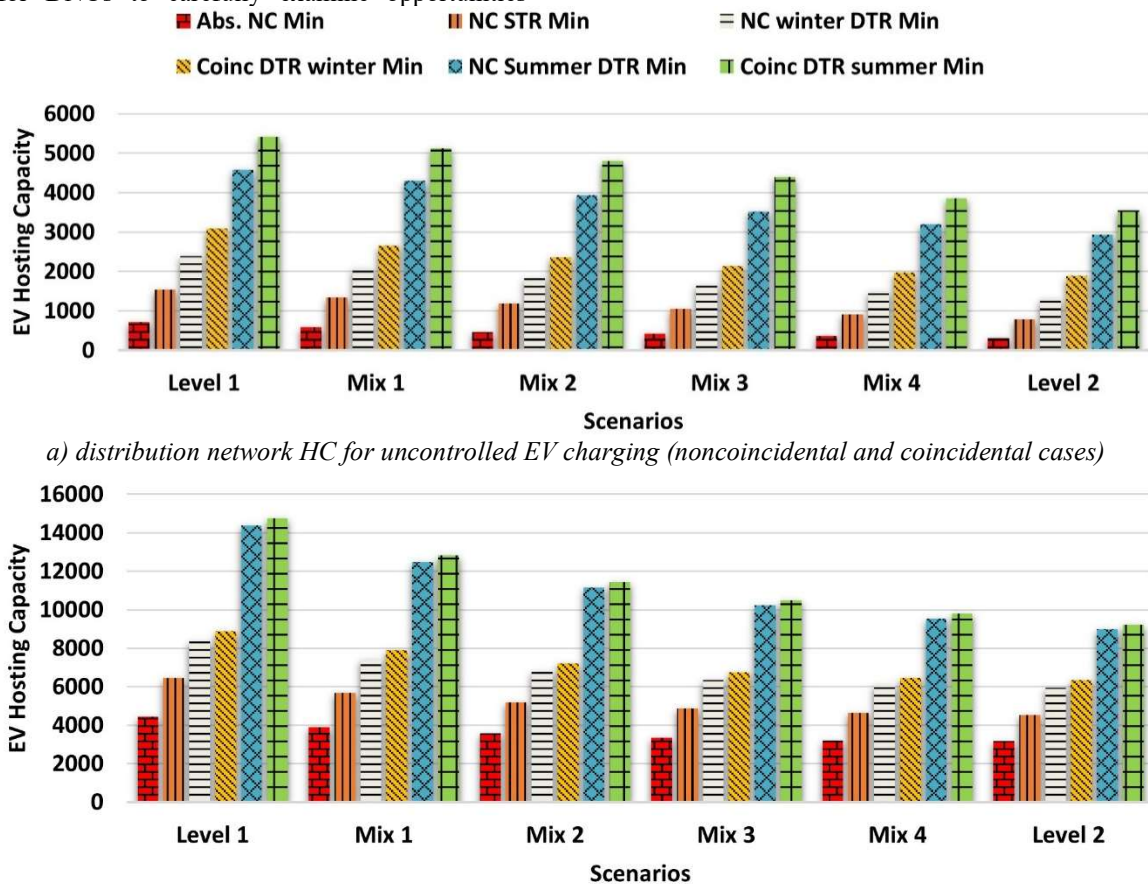


Fig.20 Network EV HC results: a) firm EV HC (uncontrolled EV charging), and b) non-firm HC (controlled EV charging)

## 8. Conclusions

This paper presented a simple yet robust methodology to determine the range of HC of distribution networks for controlled and uncontrolled residential EV charging, using both static and dynamic thermal ratings (STRs and DTRs) of network components. In order to produce realistic results of the analysis, the methodology is illustrated using UK-based uncontrolled EV charging load profiles and typical UK residential pre-EV demands, as well as weather data from a UK weather station. However, the presented methodology can be easily applied to other countries/locations/climates by providing required corresponding data. For example, in a country with a hot climate, where peak annual demand occurs in summer (e.g., due to electric cooling loads), coinciding with the minimum DTR values, the HC for EV charging may

be significantly lower than in a country with cold climate, where the peak annual demand occurs in winter (e.g. in the UK, due to electric heating loads). The EV charging demands may be also different in summer and in winter (additional discharging of EV batteries for cooling/air-conditioning).

The presented methodology allows to evaluate one commonly used network design parameter, ADMD, but also introduces per-hour ADMD values and MDED as the new and useful parameters for evaluating network EV HC for uncontrolled and controlled (scheduled) EV charging. In particular, the MDED allows to directly calculate the maximum number of EVs that can be safely connected (without overloading network components) in fully controlled EV charging mode, based on the available network supply capacity (difference between the applied thermal

limits and pre-EV load profile on the day of maximum demand).

The presented results for uncontrolled EV charging are obtained by applying probabilistic Monte Carlo simulations on the available EV charging data from a UK field trial. Both Level 1 (older) and Level 2 (newer) EV chargers are included in the analysis, as well as their mixes. A direct comparison of obtained daily EV charging profiles with typical UK residential load profiles (pre-EV load) confirmed that their respective maximum demands occur at different times of the day, suggesting that conventional (single) ADMD values cannot be used for the correct evaluation of the impact of increasing number of EVs on LV and MV networks. Instead of the single ADMD value, hourly ADMD values, obtained from the maximum EV charging demands, should be combined with hourly maximum pre-EV load demands for assessing total maximum demands.

Amongst a large number of all possible EV charging control schemes, the presented analysis introduces one particular EV scheduling strategy, which calculates the maximum number of EVs that can be hosted in a given network, with given pre-EV load demand and given loading limit of network components. Similar analysis could be done for analysing effects and impact of the anticipated electrification of heating, e.g., replacement of natural gas heating with heat pumps and other electric thermal loads.

## 9. References

- [1] N. Panossian, M. Muratori, B. Palmintier, A. Meintz, T. Lipman, and K. Moffat, "Challenges and Opportunities of Integrating Electric Vehicles in Electricity Distribution Systems," *Curr. Sustain. Energy Reports*, vol. 9, no. 2, pp. 27–40, 2022.
- [2] A. S. Al-Ogaili *et al.*, "Review on scheduling, clustering, and forecasting strategies for controlling electric vehicle charging: Challenges and recommendations," *IEEE Access*, vol. 7, pp. 128353–128371, 2019.
- [3] S. K. Rathor and D. Saxena, "Energy management system for smart grid: An overview and key issues," *Int. J. Energy Res.*, no. April 2019, pp. 1–43, 2020.
- [4] M. Alturki and A. Khodaei, "Marginal Hosting Capacity Calculation for Electric Vehicle Integration in Active Distribution Networks," *Proc. IEEE Power Eng. Soc. Transm. Distrib. Conf.*, vol. 2018-April, 2018.
- [5] E. C. Da Silva, O. D. Melgar-Dominguez, and R. Romero, "Simultaneous distributed generation and electric vehicles hosting capacity assessment in electric distribution systems," *IEEE Access*, vol. 9, pp. 110927–110939, 2021.
- [6] J. Zhao, J. Wang, Z. Xu, C. Wang, C. Wan, and C. Chen, "Distribution Network Electric Vehicle Hosting Capacity Maximization: A Chargeable Region Optimization Model," *IEEE Trans. Power Syst.*, vol. 32, no. 5, pp. 4119–4130, 2017.
- [7] X. Gong, T. Lin, and B. Su, "Impact of plug-in hybrid electric vehicle charging on power distribution network," *Dianwang Jishu/Power Syst. Technol.*, vol. 36, no. 11, pp. 30–35, 2012.
- [8] R. C. Green, L. Wang, and M. Alam, "The impact of plug-in hybrid electric vehicles on distribution networks: A review and outlook," *Renew. Sustain. Energy Rev.*, vol. 15, no. 1, pp. 544–553, 2011.
- [9] H. S. Salama, S. M. Said, I. Vokony, and B. Hartmann, "Impact of Different Plug-in Electric Vehicle Categories on Distribution Systems," *7th Int. Istanbul Smart Grids Cities Congr. Fair, ICSG 2019 - Proc.*, pp. 109–113, 2019.
- [10] Y. Ma, B. Zhang, and X. Zhou, "An overview on impacts of electric vehicles integration into distribution network," *2015 IEEE Int. Conf. Mechatronics Autom. ICMA 2015*, pp. 2065–2070, 2015.
- [11] J. Love *et al.*, "The addition of heat pump electricity load profiles to GB electricity demand: Evidence from a heat pump field trial," *Appl. Energy*, vol. 204, pp. 332–342, 2017.
- [12] Z. Wang, J. Crawley, F. G. N. Li, and R. Lowe, "Sizing of district heating systems based on smart meter data: Quantifying the aggregated domestic energy demand and demand diversity in the UK," *Energy*, vol. 193, 2020.
- [13] C. Barteczko-Hibbert, "After Diversity Maximum Demand (ADMD) Report. Customer-Led Network Revolution," pp. 334–334, 2015, [Online]. Available: [http://www.eon.uk.com/downloads/network\\_design\\_manual.pdf](http://www.eon.uk.com/downloads/network_design_manual.pdf)
- [14] C. Crozier, T. Morstyn, and M. McCulloch, "Capturing diversity in electric vehicle charging behaviour for network capacity estimation," *Transportation Research Part D: Transport and Environment*, vol. 93, 2021.
- [15] S. Ali, P. Wintzek, and M. Zdrallek, "Development of Demand Factors for Electric Car Charging Points for Varying Charging Powers and Area Types," *Electricity*, vol. 3, no. 3, pp. 410–441, 2022.
- [16] J. Bollerslev *et al.*, "Coincidence Factors for Domestic EV Charging from Driving and Plug-In Behavior," *IEEE Trans. Transp. Electrification*, vol. 8, no. 1, pp. 808–819, 2022.
- [17] I. Daminov, A. Prokhorov, R. Caire, and M. C. Alvarez-Herault, "Assessment of dynamic transformer rating, considering current and temperature limitations," *Int. J. Electr. Power Energy Syst.*, vol. 129, no. August 2020, 2021.
- [18] D. L. Alvarez, S. R. Rivera, S. Member, E. E. Mombello, and S. Member, "Prediction Using Dynamic Rating Monitoring," *IEEE Trans. Power Deliv.*, vol. 34, no. 4, pp. 1695–1705, 2019.
- [19] "IEEE Guide for Loading Mineral-Oil-Immersed Transformers and Step-Voltage Regulators." in IEEE Guide for Loading Mineral-Oil-Immersed Transformers. IEEE, pp. 1–123, 2012.
- [20] V. Shiravand, J. Faiz, M. H. Samimi, and M. Djmalali, "Improving the transformer thermal modeling by considering additional thermal points," *Int. J. Electr. Power Energy Syst.*, vol. 128, no. December 2020, 2021.
- [21] S. Talpur, T. T. Lie, R. Zamora, and B. P. Das, "Maximum utilization of dynamic rating operated distribution transformer (DRoDT) with battery energy storage system: Analysis on impact from battery electric vehicles charging," *Energies*, vol. 13, no. 13, 2020, doi: 10.3390/en13133411.
- [22] B. C. Blake-Coleman and R. Yorke, "Faraday and Electrical Conductors - an Examination of the Copper Wire Used By Michael Faraday Between 1821 and 1831.," *IEE Proc. A Phys. Sci. Meas. Instrumentation. Manag. Educ. Rev.*, vol. 128, no. 6, pp. 463–471, 1981.
- [23] S. Karimi, P. Musilek, and A. M. Knight, "Dynamic thermal rating of transmission lines: A review," *Renew. Sustain. Energy Rev.*, vol. 91, no. August 2016, pp. 600–612, 2018.
- [24] M. Bunn, B. C. Seet, C. Baguley, and D. Martin, "A Thermally-Based Dynamic Approach to the Load Management of Distribution Transformers," *IEEE Trans. Power Deliv.*, vol. 37, no. 6, pp. 5124–5132, 2022.
- [25] B. Alharbi and D. Jayaweera, "Impact Assessment of Plug-in Electric Vehicle Charging Locations on Power Systems with Integrated Wind Farms Incorporating Dynamic Thermal Limits," *J. Mod. Power Syst. Clean Energy*, vol. 10, no. 3, pp. 710–718, 2022.
- [26] J. C. Mukherjee and A. Gupta, "A Review of Charge Scheduling of Electric Vehicles in Smart Grid," *IEEE Syst. J.*, vol. 9, no. 4, pp. 1541–1553, 2015.
- [27] Z. Yang, K. Li, and A. Foley, "Computational scheduling methods for integrating plug-in electric vehicles with power systems: A review," *Renew. Sustain. Energy Rev.*, vol. 51, pp. 396–416, 2015.
- [28] Y. Zheng, S. Niu, Y. Shang, Z. Shao, and L. Jian, "Integrating plug-in electric vehicles into power grids: A comprehensive review on power interaction mode, scheduling methodology and mathematical foundation," *Renew. Sustain. Energy Rev.*, vol. 112, no. January, pp. 424–439, 2019, doi: 10.1016/j.rser.2019.05.059.
- [29] D. Liu, P. Zeng, S. Cui, and C. Song, "Deep Reinforcement Learning for Charging Scheduling of Electric Vehicles Considering Distribution Network Voltage Stability," *Sensors*, vol. 23, no. 3, 2023.
- [30] W. Sun, F. Neumann, and G. P. Harrison, "Robust Scheduling of Electric Vehicle Charging in LV Distribution Networks under Uncertainty," *IEEE Trans. Ind. Appl.*, vol. 56, no. 5, pp. 5785–5795, 2020.
- [31] J. Yang, J. Xiong, Y.-L. Chen, P. L. Yee, C. S. Ku, and M. Babanezhad, "Improved Golden Jackal Optimization for Optimal Allocation and Scheduling of Wind Turbine and Electric Vehicles Parking Lots in Electrical Distribution Network Using Rosenbrock's Direct Rotation Strategy," *Mathematics*, vol. 11, no. 6, p. 1415, 2023.
- [32] A. Zakaria, F. B. Ismail, M. S. H. Lipu, and M. A. Hannan, "Uncertainty models for stochastic optimization in renewable

- energy applications,” *Renewable Energy*, vol. 145, pp. 1543–1571, 2020.
- [33] D. Fang *et al.*, “Deterministic and Probabilistic Assessment of Distribution Network Hosting Capacity for Wind-Based Renewable Generation,” in *2020 International Conference on Probabilistic Methods Applied to Power Systems (PMAPS)*, Aug. 2020, pp. 1–6.
- [34] E. V Registrations, C. Eligible, F. O. R. The, and P. C. A. R. Grant, “My Electric Avenue,” 2017.
- [35] E. D. Org, “Nissan Leaf Electric Vehicle Database.” <https://ev-database.org/uk/car/1019/Nissan-Leaf-24-kWh>
- [36] K. Joshi and A. Lakum, “Assessing the impact of Plug-in Hybrid Electric Vehicles on distribution network operations using Time-Series Distribution Power Flow analysis,” *2014 IEEE Int. Conf. Power Electron. Drives Energy Syst. PEDES 2014*, 2014.
- [37] Baran; Wu, “Network Reconfiguration in Distribution Systems for Loss Reduction and Load Balancing,” *IEEE Trans. Power Deliv.*, vol. 4, no. 2, pp. 1401–1406, 1989.
- [38] [www.elandcables.com](http://www.elandcables.com), “ACSR - ASTM - B Aluminium Conductor Steel Reinforced,” pp. 1–10, 2014.
- [39] Z. ABB Zhongshan Transformer Company Ltd., “Technical specification SZ13-6300/35.”
- [40] A. Molod, L. Takacs, M. Suarez, and J. Bacmeister, “Development of the GEOS-5 atmospheric general circulation model: evolution from MERRA to MERRA2,” *Geosci. Model Dev.*, vol. 8, no. 5, pp. 1339–1356, 2015.
- [41] *IEEE Std 738-1993: IEEE Standard for Calculating the Current-Temperature Relationship of Bare Overhead Conductors*. IEEE, 1993.
- [42] C. M. Lai and J. Teh, “Comprehensive review of the dynamic thermal rating system for sustainable electrical power systems,” *Energy Reports*, vol. 8, pp. 3263–3288, 2022.
- [43] Northern Powergrid, “Code of Practice for Overhead Line Ratings and Parameters,” 2017.
- [44] I. Hernando Gil, “Integrated assessment of quality of supply in future electricity networks,” *PhD’s thesis, Univ. Edinburgh*, pp. 1–261, 2014.
- [45] GOV.UK, “National Travel Survey 2021: Household car availability and trends in car trips,” 2022. <https://www.gov.uk/government/statistics/national-travel-survey-2021/national-travel-survey-2021-household-car-availability-and-trends-in-car-trips>
- [46] R. D. Zimmerman, C. E. Murillo-Sánchez, and R. J. Thomas, “MATPOWER: Steady-State Operations, Planning, and Analysis Tools for Power Systems Research and Education,” *IEEE Trans. Power Syst.*, vol. 26, no. 1, pp. 12–19, Feb. 2011.